A Maritime Multi-User GBSM for Land-to-Ship Communications

Pingfan Su[1], Hengtai Chang[2,1 *], Cheng-Xiang Wang[1,2 *], Yilin Ma[1,2], Jie Huang[1,2], and Yubei He[3]
[1]National Mobile Communications Research Laboratory, School of Information Science and Engineering, Southeast University, Nanjing 210096, China.
[2]Pervasive Communication Research Center, Purple Mountain Laboratories, Nanjing 211111, China.
[3]Department of Engineering, Durham University, Durham, DH1 3LE, UK.
[*]Corresponding Authors
Email: 220220969@seu.edu.cn, changhengtai@pmlabs.com.cn,
{chxwang, yilin_ma, j_huang}@seu.edu.cn, yubei.he@durham.ac.uk

***Abstract*—In this paper, a geometry-based stochastic model (GBSM) is proposed for multiple-input multiple-output (MIMO) maritime multi-user land-to-ship communication channels. The inter-link correlation between different users is modeled by spatial correlated large scale parameters (LSPs). In addition, the evaporation duct is modeled based on a twin-cluster model, and the signal propagation between two clusters is simulated by several-order reflections to obtain the delay and angle parameters of each ray. Simulations based on the proposed model focus on analyzing the statistical properties that reflect the spatial correlation between multiple users. Effects of the number of antennas, multipath components (MPCs), and different heights of evaporation duct on the correlation between users and the channel capacity are investigated and corresponding conclusions are drawn.**

***Index Terms*—Maritime land-to-ship communication, multi-user channel, evaporation duct, GBSM, spatial correlation.**

I. Introduction

Maritime communication has been an integral part of the sixth-generation wireless communication system to achieve global coverage in recent years [1], [2]. In the meantime, with the rapid development of marine economy, maritime communication technology also requires improvement to meet the requirements of transmission rate, accuracy, and latency of communication systems in maritime activities. To meet the future requirements of maritime communication systems, characteristics of maritime communication channels should be deeply researched.

Therefore, maritime multi-user channel is well worth investigating, but current researches are mainly about single-user channel. In current research, maritime communication channel characteristics which are mainly researched include sparse scattering, sea wave movement and evaporation duct phenomenon [3]. Evaporation duct has received widespread attention due to its ability of providing trans-horizon transmission. Many channel measurements and modeling have been carried out around evaporation duct. In [4]–[7], the path loss of evaporation duct propagation over the sea was measured under different conditions such as different evaporation duct heights, different transmit frequencies, and different climate conditions. Doppler shift, delay power spectral density (PSD), and K-factor were also measured in [7]. Authors in [8], [9] developed large-scale path loss models for the evaporation ducts. In [8], authors also analyzed the delay spread and angle of arrival (AoA) of the ducting channel. Models mentioned above are mostly deterministic models. Because GBSMs can provide a good balance between computation complexity and accuracy compared to deterministic models [10], [11], these modeling methods have been widely used in the development of maritime channel models [12], [13]. In [14], a novel three-dimensional (3D) GBSM for maritime ship-to-ship communication channel was proposed and the evaporation duct was modeled by the method of twin-cluster GBSM. For maritime multi-user channel, authors in [15] proposed an integrated sensing and communication base station system designed for applications by multiple users in maritime environments. However, effects of maritime communication channel characteristics on the correlation between users were not studied.

To fill the gaps in current research, a maritime multi-user land-to-ship GBSM is proposed in this paper. The evaporation duct in maritime communication scenario is considered and modeled. The correlation between different users is modeled by spatial correlated LSPs and the interference between users is also modeled. Effects of the number of antennas, multipath components, and different heights of evaporation duct on correlation between different users and channel capacity are investigated based on this model.

The rest of this paper is organized as follows. The maritime multi-user land-to-ship channel model is described in Section II. LSPs and small scale parameters (SSPs) are modeled and the evaporation duct model is illustrated. In Section III, channel characteristics including channel matrix collinearity (CMC), spatial cross-correlation functions (CCF), and the channel capacity are derived. Simulation results are presented and corresponding analyses in Section IV. Finally, conclusions are drawn in Section V.

II. A Maritime Multi-user Channel Model

A. The 3D Multi-User Land-to-Ship MIMO Channel Model

In this proposed model, the uniform circle array (UCA) is mounted and fixed on the shore as Tx, and the uniform linear array (ULA) is equipped on board and move with the ship as Rx. The complete channel impulse response (CIR) matrix of the channel can be denoted as

$$\mathbf{H} = [PL \cdot SH]^{\frac{1}{2}} \cdot \mathbf{H_s} \tag{1}$$

where *PL* represents the path loss in propagation. Shadow fading is denoted as *SH*. Here, $\mathbf{H_s} = [h_{pq}(t,\tau)]_{N_T \times N_R}$ represents the CIR of small-scale fading, where $h_{pq}(t,\tau)$ is the CIR of the fading channel between the p-th Tx antenna element and q-th Rx antenna element, N_T and N_R are the total number of the transmitting and receiving antennas, respectively.

In multi-user communication scenario, the received signal of user k can be represented as

$$\mathbf{Y}_k = \sqrt{\rho}\mathbf{H_{C}}_k\mathbf{X_{C}}_k + \sqrt{\eta}\mathbf{H_I}\mathbf{X_I} + n \tag{2}$$

where $\mathbf{H_{C}}_k$ and $\mathbf{X_{C}}_k$ denote the normalized channel matrix and transmit signal of user k, respectively. The symbols ρ and η are used to denote the signal-to-noise ratio (SNR) and interference-to-noise ratio (INR), respectively. The symbol n denotes the noise matrix. Similarly, $\mathbf{H_I}$ and $\mathbf{X_I}$ denote the normalized channel matrix and signal of interference link, respectively. Here, $\mathbf{H_I X_I}$ can be calculated as $\sum_{u=1,u\neq k}^{N} H_u\mathbf{X}_u$, where N is the total numbers of users, $\mathbf{H}_u$ and $\mathbf{X}_u$ are the channel matrix and interference signal of user u, respectively. The proposed model consists of the LoS component, sea surface scattering component, and evaporation duct propagation component as illustrated in Fig. 1.

Based on the model described above, $h_{pq}(t,\tau)$ can be determined by summing over all components in channel, i.e.,

$$\begin{aligned} h_{pq}(t,\tau) = \sqrt{\frac{K_R}{K_R+1}} h_{\mathrm{LoS}}^{pq}(t,\tau) + \sqrt{\frac{S_1}{K_R+1}} h_{\mathrm{NLoS}_1}^{pq}(t,\tau) \\ + \sqrt{\frac{S_2}{K_R+1}} h_{\mathrm{NLoS}_2}^{pq}(t,\tau) \end{aligned} \tag{3}$$

where K_R denotes the K-factor, $h_{\mathrm{LoS}}^{pq}(t,\tau)$ denotes the complex envelops of the LoS component, $h_{\mathrm{NLoS}_1}^{pq}(t,\tau)$ and $h_{\mathrm{NLoS}_2}^{pq}(t,\tau)$ represent the complex envelops of the sea surface scattering component and evaporation duct propagation component, respectively. Here, S_1 and S_2 are the power control factors for manipulating the appearance and disappearance of the sea level path and the evaporation duct path with the change of the ship position, and $S_1 + S_2 = 1$.

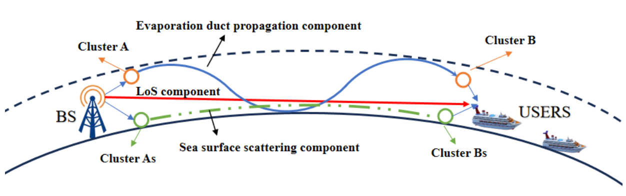

Fig. 1. Illustration of the land-to-ship communication scenario.

B. LSPs and SSPs Modeling

The LSPs of this channel model mainly contain PL, K-factor, SH, and angular spread of elevation and azimuth angles. The PL changes with the movement of ships and can be modeled as [3]

$$PL = \begin{cases} -10\log_{10}\left\{\left(\frac{\lambda}{4\pi d}\right)^2\left[2\sin\left(\frac{2\pi h_t h_r}{\lambda d}\right)\right]^2\right\}, d \le d_0 \\ -10\log_{10}\left\{\left(\frac{\lambda}{4\pi d}\right)^2[2(1+\Delta)]^2\right\}, d_0 < d < d_{\mathrm{bLoS}} \\ A - \frac{10\gamma\log d}{d_{\mathrm{bLoS}}}, d_{\mathrm{bLoS}} < d \end{cases} \tag{4}$$

where $\Delta = 2\sin\left(\frac{2\pi h_t h_r}{\lambda d}\right)\sin\left(\frac{2\pi(h_e-h_t)(h_e-h_r)}{\lambda d}\right)$, $A = -10\log_{10}\left\{\left(\frac{\lambda}{4\pi d_{\mathrm{bLoS}}}\right)^2[2(1+\Delta)]^2\right\}$, h_t, h_r, and h_e are the heights of the Tx, Rx, and evaporation duct, respectively. Here, γ denotes the path-loss exponent, and λ is the wavelength of the signal. The distance between Rx and Tx is represented as d, and $d_0 = \frac{4h_t h_r}{\lambda}$ denotes the maximum distance between Rx and Tx that only the paths from LoS and sea surface scattering in the propagation can arrive at the receiving antennas. Besides, $d_{\mathrm{bLoS}} = \sqrt{h_t^2 + 2R_e h_t} + \sqrt{h_r^2 + 2R_e h_r}$ is the distance beyond which LoS path will disappear, where R_e is the radius of the earth. When d exceeds d_{bLoS}, only the paths from evaporation duct are involved.

Considering the multi-user land-to-ship communication scenario, different ships can be regarded as multiple users with different locations. Their propagation path loss varies with their distances to the base station. The other LSPs will also change accordingly due to the motion of Rx and location. However, LSPs will remain constant at adjacent positions according to the spatial consistency theory. Thus the range of antenna motions and multi-user positions can be divided into many grids. In order to ensure that the LSPs of different grids are correlated, an exponential spatial filter [16] can be adopted to generate the LSPs. The exponential spatial filter could be expressed as [14]

$$\tilde{g}_{a,b} = \sum_{x=0}^{G_x}\sum_{y=0}^{G_y} g_{x,y} f(a-x, b-y) \tag{5}$$

where $\tilde{g}_{a,b}$ and $g_{x,y}$ denote the spacial correlated LSPs and original uncorrelated LSPs, respectively. The product of G_x and G_y is the total number of the grids. Here, $f(a-x, b-y)$ is the exponential filter defined as

$$f(a-x, b-y) = \exp\left(-\frac{D_g\|a-x, b-y\|}{D_c^S}\right) \tag{6}$$

where D_g and D_c^S are the side length of grids and correlated distance in the time domain, respectively.

SSPs consist of the power, angle, and phase of each ray. The angular parameters of the LoS path can be determined from the coordinates of Tx and Rx. For the paths caused by the sea surface scattering, the angular parameters can be generated from a truncated Gaussian distribution [17]. The angular parameters in turn can be combined with the antenna coordinates to generate the positions of the clusters beside Tx and Rx. The time-variant ray power can be calculated according to a single slope exponential power delay profile [18]. The survival and disappearance of clusters in this model is suitable for description by the Poisson processes. The exact formulas and calculation processes can be found in [9].

C. The Evaporation Duct Modeling

Evaporation duct is crucial for its high probability of occurrence and the ability of providing trans-horizon transmission. As illustrated in Fig. 2, since the evaporation duct is close to the ocean surface, the propagation channel between cluster A (cluster of Tx side) and cluster B (cluster of Rx side) can be abstracted as a waveguide between two parallel surfaces. The upper plane is the evaporation duct and the other plane is the sea surface. The coordinate of cluster A is set as $(x_A(t), y_A(t), z_A(t))$, and the coordinate of cluster B is denoted by $(x_B(t), y_B(t), z_B(t))$. r_p denotes that $p+1$ times reflection occurred between the two planes.

The distance of signal propagation between cluster A and B is denoted as $d_{I_p}(t)$ and can be calculated as

$$d_{I_p}(t) = \sqrt{\left(d^x_{I_p}(t)\right)^2 + \left(d^y_{I_p}(t)\right)^2 + \left(d^z_{I_p}(t)\right)^2} \tag{7a}$$

$$d^x_{I_p}(t) = x_B(t) - x_A(t) \tag{7b}$$

$$d^y_{I_p}(t) = y_B(t) - y_A(t) \tag{7c}$$

$$d^z_{I_p}(t) = \begin{cases} ph_e + z_A(t) + z_B(t), & \text{p is odd} \\ (p+1)h_e + z_A(t) - z_B(t), & \text{p is even} \end{cases} \tag{7d}$$

According to $d_{I_p}(t)$, the delay between cluster A and B can be calculated as

$$\tau_{AB} = \frac{d_{I_p}(t)}{\lambda f} \tag{8}$$

where f and λ represent the frequency and wavelength of the signal. Due to the number of reflections must be an integer, p has to satisfy the equations

$$p = \begin{cases} \frac{\tan\alpha}{h_e}\sqrt{\left(d^x_{I_p}(t)\right)^2 + \left(d^y_{I_p}(t)\right)^2} - \frac{1}{h_e}\left(z_A(t) - z_B(t)\right) \\ \qquad = \text{odd} \\ \frac{\tan\alpha}{h_e}\sqrt{\left(d^x_{I_p}(t)\right)^2 + \left(d^y_{I_p}(t)\right)^2} - \frac{1}{h_e}\left(z_A(t) + z_B(t)\right) \\ \qquad -1 = \text{even} \end{cases} \tag{9}$$

where α is the elevation angle, of which maximum and minimum values can be calculated as [14]

$$\alpha^T_{\text{max,min}} = \pm\sqrt{2\left(\frac{1}{n(0)}\frac{dn(z)}{dz}\bigg|_{z=h_e} + \frac{1}{R_e}\right)(h_T - h_e)} \tag{10}$$

where $n(0)$ denotes the refractive index at the sea surface. The refractive index function $n(z)$ which denotes the vertical height off the sea surface. $\frac{dn(z)}{dz}$ can be represented as [14]

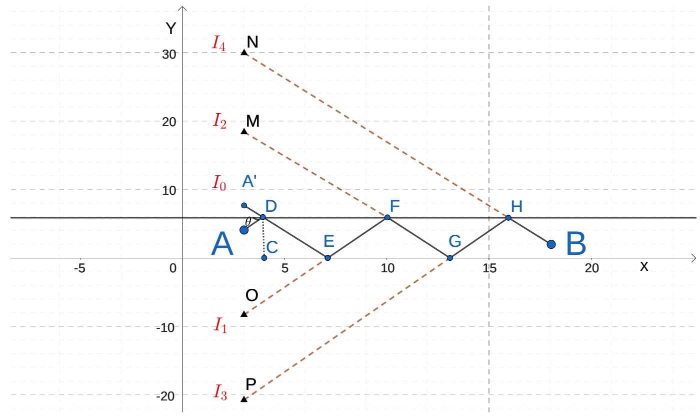

Fig. 2. Reflections between the sea level and the evaporation duct.

$$\frac{dn(z)}{dz} = \left(\frac{dM(z)}{dz} - 0.157\right) \times 10^{-6} \tag{11}$$

where $M(z) = M_0 + 0.125z - 0.125h_e ln(\frac{z+z_0}{z_0})$ represents the modified refractivity profile in evaporation duct. $M_0 = 315$ M-units, and $z_0 = 1.5 \times 10^{-4}$ m. According to the value of $\alpha^T_{\text{max,min}}$ and the formula (9), the angular parameters of the evaporation duct propagation component can be determined.

III. Analysis of Multi-user Channel Properties

A. CMC

The CMC can describe the spatial structure similarity of two matrices with the same dimensions [19]. Assuming that the channel matrices of two users represented as u_1 and u_2 are $\mathbf{H}(u_1)$ and $\mathbf{H}(u_2)$, respectively. Then, the CMC between u_1 and u_2 can be defined as [11]

$$\eta(u_1, u_2) = \mathbb{E}\left\{\frac{\text{tr}\left\{\mathbf{H}(u_1)^{\text{H}}\mathbf{H}(u_2)\right\}}{\|\mathbf{H}(u_1)\|_{\text{F}}\|\mathbf{H}(u_1)\|_{\text{F}}}\right\} \tag{12}$$

where $tr(\cdot)$ is the operation for calculating matrix trace. $(\cdot)^{\text{H}}$ represents conjugate operation, $\|\cdot\|_{\text{F}}$ denotes the Frobenius norm. The value range of the CMC is $(0, 1)$. Channel correlation between users increases with CMC. When the CMC takes 0, it means that the channels between users are completely uncorrelated because their channel matrices have no linear relationship. On the contrary, when the CMC is 1, it means that the channels between users are highly correlated.

B. Spatial CCF

Spatial domain is used to describe a MIMO channel from the p-th $(p = 1, 2, ..., P)$ Tx element to the q-th $(q =$

$1, 2, \ldots, Q$) Rx element. The spatial CCF, which represents the spatial cross correlation of channel, can be defined as

$$R_{pq,p'q'}(t,f;\Delta\xi) = \frac{K_R}{K_R+1} R^{\mathrm{LoS}}_{pq,p'q'}(t,f;\Delta\xi) + \frac{1}{K_R+1}\left[\sum_{n_1=1}^{N_1^{pq}(t)} R^{\mathrm{NLoS}_1}_{pq,p'q',n_1}(t,f;\Delta\xi) + \sum_{n_2=1}^{N_2^{pq}(t)} R^{\mathrm{NLoS}_2}_{pq,p'q',n_2}(t,f;\Delta\xi)\right] \quad (13)$$

where $\Delta\xi = \{\Delta\xi_T, \Delta\xi_R\}$, $\Delta\xi_T$ and $\Delta\xi_R$ are the antenna spacing of transmitting and receiving antennas, respectively. $R^{\mathrm{LoS}}_{pq,p'q'}$, $R^{\mathrm{NLoS}_1}_{pq,p'q',n_1}$, and $R^{\mathrm{NLoS}_2}_{pq,p'q',n_2}$ are the correlation functions of the components from LoS, sea surface scattering, and evaporation duct propagation, respectively.

C. Channel Capacity and Channel Relative Capacity

Channel capacity refers to the maximum rate at which a channel can transmit information without error. It establishes the basic limit of reliable communication and is widely used to measure the performance of communication systems. Considering the interference among different users, the ergodic channel capacity can be calculated as [20]

$$C_{\mathbf{H_C},\mathbf{H_I}} = \mathbb{E}\left\{\log_2\left[\det\left(\mathbf{I} + \frac{\rho}{M}\mathbf{H}_C^T\mathbf{H}_C^*\mathbf{R_I}^{-1}\right)\right]\right\} \quad (14)$$

$$\rho = \frac{P_s \cdot PL \cdot \lambda_{max}\left(\mathbf{H_C}\mathbf{H_C^H}\right)}{N_0} \quad (15)$$

where P_s is the signal transmission power, λ_{max} represents the maximum singular value, $\mathbf{R_I}$ is the instantaneous covariance matrix and can be expressed as

$$\mathbf{R_I} = \eta\mathbf{H_I}\mathbf{H_I}^* + \mathbf{I}. \quad (16)$$

The ergodic capacity ratio in the presence and absence of inter-user interference can be expressed in terms of relative capacity (RC), which in turn measures the impact of the interference from different users on channel capacity. Thus, from the clarification above, RC can be defined as [20]

$$RC = \frac{C_{\mathbf{H_C},\mathbf{H_I}} + C_{\mathbf{H_I},\mathbf{H_C}}}{C_{\mathbf{H_C}} + C_{\mathbf{H_I}}}. \quad (17)$$

The value of the channel relative capacity is $(0, 1)$. A larger RC indicates that the inter-user interference has less influence on the relative capacity and therefore the channel correlation between different users is lower.

IV. Results and Analysis

Simulation results of the multi-user land-to-ship channel model are presented and the analysis of the results follows in this section. The correlation characteristics of multi-user channels are mainly focused in the simulation work. Main simulation parameters are listed here: Tx height $h_t = 15$ m, Rx height $h_r = 6$ m, carrier frequency $f_c = 5.8$ GHz, speed of ship $v = 10$ m/s, user interval $\delta_d = 20$ m. UCA and ULA are equipped with 64 antenna elements and 4 antenna elements in the Tx and Rx side, respectively. The correlation distance of LSPs is set as $D_c = 100$ m.

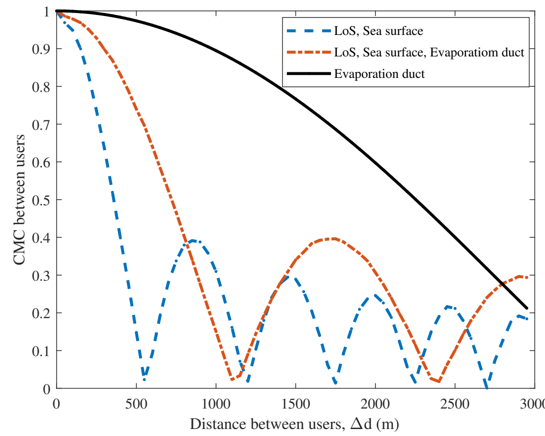

Fig. 3. Multi-user CMC with different components ($K_R = 18.1$ dB, $h_e = 25$ m, $d_u = 10^{-3}/\mathrm{m}^2$).

Fig. 3 shows the CMC with different components. When the distance d between Tx and Rx varies by a certain amount, the multipath components are also different. The distance d takes 4000 m, 9000 m and 20000 m respectively, which represents the LoS component and sea surface scattering component, all the three components consisting of the LoS component, sea surface scattering component, and evaporation waveguide propagation components, and only the evaporation waveguide propagation components.

As shown in Fig. 3, the CMC decreases in a fluctuating trend as the user distance increases, which is because the correlation between channels of different user is lower when the users are far away. The CMC increases with the increase of d, which represents that the channels of different users have higher correlation. This is because the increase of distance between Tx and Rx makes the channel multipath angle parameters of different users closer.

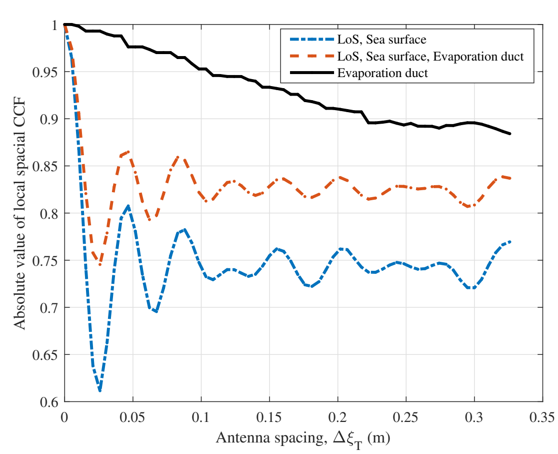

Fig. 4. Spatial CCF with different components ($K_R = 18.1$ dB, $h_e = 25$ m, $d_u = 10^{-3}/\mathrm{m}^2$).

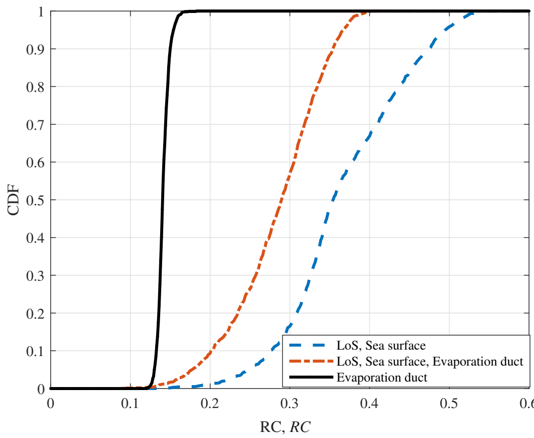

Fig. 5. Channel RC with different components ($K_R = 18.1$ dB, $h_e = 25$ m, $d_u = 10^{-3}/\mathrm{m}^2$).

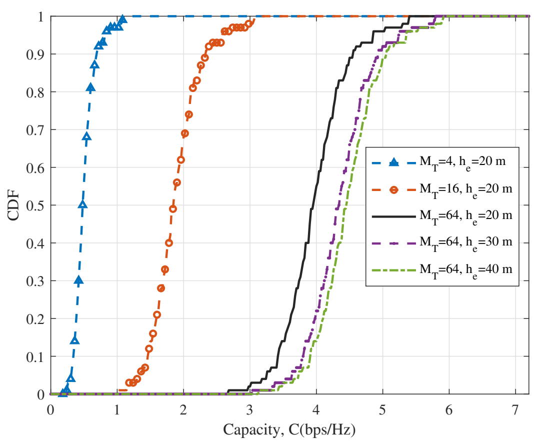

Fig. 6. Channel capacity with different evaporation duct heights and antenna numbers ($K_R = 18.1$ dB, $d_u = 10^{-3}/\mathrm{m}^2$).

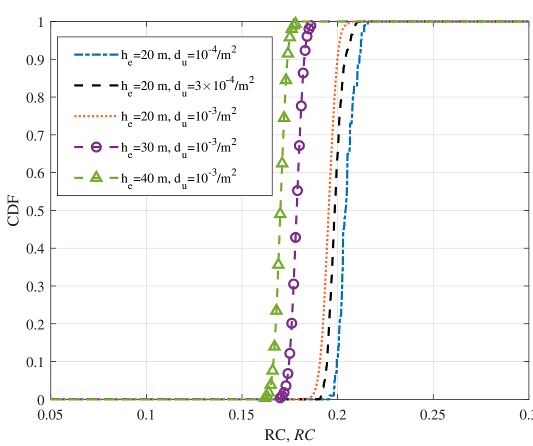

Fig. 7. Channel RC with different user densities and evaporation duct heights ($K_R = 18.1$ dB, $M_T = 16$).

Fig. 4 shows the variation of spatial CCF with antenna elements spacing and compares the absolute value of spacial CCFs with different components. According to the figure, it can be concluded that the absolute value of spacial CCFs increases with d, correspondingly, indicating that the similarity of the channels increases. This is consistent with the conclusion drawn in Fig. 3. The relative channel capacity distribution under different multipath components is shown in Fig. 5. The relative capacity of the channel decreases when the channel multipath component changes from containing only LoS component and sea surface scattering component to containing all three components to only containing evaporation duct propagation component. This also indicates a higher degree of linearity between channels of different users, which is the same conclusion as shown in Fig. 3 and Fig. 4.

In Fig. 6, the channel capacity cumulative distribution functions (CDF) for different antenna element numbers and different evaporation duct heights are compared. The channel capacity increases with the evaporation duct height according to the figure, because raising the evaporation duct height can increase the maximum capture angle of the channel, which enables the channel to capture more energy. The path loss will decrease with more signal energy captured, thus the SNR will increase. The decrease rate of path loss will gradually slow down with the evaporation duct height increasing. From Fig. 6, it can be found that the channel capacity increases significantly with the number of transmitter antennas. The reason is that increasing the number of antennas increases the spatial multiplexing rate, which in turn extends the spatial degrees of freedom of the channel.

Fig. 7 provides the CDF of channel RC with different user densities and evaporation duct heights. From Fig. 7 we can find that the channel RC decreases as the user densities increase, and this is because higher user density will increase the interference between users, thus reducing RC performance. Fig. 7 also presents that the channel RC decreases as the height of evaporation duct increases, which represents that the similarity of channels between different users increases. This is because when the height of evaporation duct increases, the power of interference signal increases correspondingly, thus improving the interference between different users.

V. Conclusions

This paper has proposed a maritime multi-user MIMO land-to-ship communication channel model. The evaporation duct has been modeled and the multi-user correlation has been investigated. Based on the proposed channel model, the CMC, spatial CCF and RC have been derived and simulated with different influencing factors. According to the simulations, increasing the distance between Tx and Rx will increase the correlation between multi-user channels. Increasing the height of the evaporation duct will increase the correlation between multi-user channels and reduce the channel capacity.

Acknowledgment

This work was supported by the National Natural Science Foundation of China (NSFC) under Grant 61960206006 and 62301365, the Fundamental Research Funds for the Central Universities under Grant 2242022k60006, the Key Technologies R&D Program of Jiangsu (Prospective and Key Technologies for Industry) under Grants BE2022067 and BE2022067-1, and the EU H2020 RISE TESTBED2 project under Grant 872172.

REFERENCES

[1] C.-X. Wang, J. Huang, H. Wang, X. Gao, X. You, and Y. Hao, "6G wireless channel measurements and models: Trends and challenges," *IEEE Veh. Technol. Mag.*, vol. 15, no. 4, pp. 22–32, Dec. 2020.

[2] C.-X. Wang, X. You, X. Gao, *et al.*, "On the road to 6G: Visions, requirements, key technologies and testbeds," *IEEE Commun. Surveys Tuts.*, vol. 25, no. 2, pp. 905–974, 2nd Quart. 2023.

[3] J. Wang, *et al.*, "Wireless channel models for maritime communications," *IEEE Access*, vol. 6, pp. 68070—68088, Nov. 2018.

[4] G. S. Woods, A. Ruxton, C. Huddlestone-Holmes, and G. Gigan, "High-capacity, long-range, over ocean microwave link using the evaporation duct," *IEEE J. Ocean. Eng.*, vol. 34, no. 3, pp. 323–330, July 2009.

[5] Wang S, *et al.*, "Long-term over-the-horizon microwave channel measurements and statistical analysis in evaporation ducts over the Yellow Sea," *Frontiers Mar. Sci*, vol. 10, Oct. 2023.

[6] Y. Shi, K.-D. Yang, Y.-X. Yang, and Y.-L. Ma, "Experimental verification of effect of horizontal inhomogeneity of evaporation duct on electromagnetic wave propagation," *Chin. Phys. B*, vol. 24, no. 4, pp.1–9, Apr. 2015.

[7] W. Wang, R. Raulef, and T. Jost, "Fading characteristics of maritime propagation channel for beyond geometrical horizon communications in C-band," *CEAS Space J.*, vol. 11, no. 9, pp. 1–10, Dec. 2017.

[8] E. Dinc and O. B. Akan, "Channel model for the surface ducts: Largescale path-loss, delay spread, and AOA," *IEEE Trans. Antennas Propag.*, vol. 63, no. 6, pp. 2728—2738, June 2015.

[9] E. Dinc and O. B. Akan, "Beyond-line-of-sight communications with ducting layer," *IEEE Commun. Mag.*, vol. 52, no. 10, pp. 37—43, Oct. 2014.

[10] C. -X. Wang, Z. Lv, X. Gao, X. You, Y. Hao, and H. Haas, "Pervasive wireless channel modeling theory and applications to 6G GBSMs for all frequency bands and all scenarios," *IEEE Trans. Veh. Technol.*, vol. 71, no. 9, pp. 9159–9173, Sept. 2022.

[11] H. Chang, *et al.*, "A general 3-D nonstationary GBSM for underground vehicular channels," *IEEE Trans. Antennas Propag.*, vol. 71, no. 2, pp. 1804–1819, Feb. 2023.

[12] Y. Liu, C.-X. Wang, H. Chang, Y. He, and J. Bian, "A novel non-stationary 6G UAV channel model for maritime communications," *IEEE J. Sel. Areas Commun.*, vol. 39, no. 10, pp. 2992-–3005, Oct. 2021.

[13] Y. He, H. Chang, Y. Liu, W. Zhang, J. Sun, and C.-X. Wang, "A 3D GBSM for ship-to-land communications," in *Proc. ICCC*, Changchun, China, Aug. 2019, pp. 967-–972.

[14] Y. He, *et al.*, "A novel 3D non-stationary maritime wireless channel model," *IEEE Trans. Commun.*, vol. 70, no. 3, pp. 2102—2116, Mar. 2022.

[15] J. Zhang, G. Wang, H. Yang, X. Wang, B. Li, "Joint waveform design for multi-user maritime integrated sensing and communication," *Wireless Netw.*, vol. 29, no. 8, pp. 1–12, June 2023.

[16] H. Chang, *et al.*, "A novel nonstationary 6G UAV-to-ground wireless channel model with 3-D arbitrary trajectory changes," *IEEE Int. Things J.*, vol. 8, no. 12, pp. 9865—9877, June 2021.

[17] N. L. Johnson and S. Kotz, *Continuous Univariate Distributions. Boston, MA*, USA: Hougton Mifflin, 1970.

[18] Study on Channel Model for Frequencies From 0.5 to 100 GHz, document TR 38.901, V14.0.0, 3GPP, Mar. 2017.

[19] F. Kaltenberger, D. Gesbert, R. Knopp, and M. Kountouris, "Correlation and capacity of measured multi-user MIMO channels," *Proc. IEEE 19th Int. Symp. PIMRC.*, Cannes, France, Dec. 2008, pp. 1–5.

[20] H. Chang *et al.*, "Multi-user UAV channel modeling with massive MIMO configuration," in *Proc. VTC-Fall'21*, Norman, USA, Sep. 2021, pp. 1–6.